



## Efficient tool flow for 3D photovoltaic modelling<sup>☆</sup>

Tasmiat Rahman<sup>\*</sup>, Kristel Fobelets

Department of Electrical and Electronic Engineering, Imperial College London, UK



### ARTICLE INFO

#### Article history:

Received 10 November 2014  
 Received in revised form  
 12 March 2015  
 Accepted 18 March 2015  
 Available online 30 March 2015

#### Keywords:

Photovoltaic  
 Simulation  
 Lumerical FDTD  
 TCAD Sentaurus

### ABSTRACT

Performance predictions and optimisation strategies in current nanotechnology-based photovoltaic (PV) require simulation tools that can efficiently and accurately compute optical and electrical performance parameters of intricate 3D geometrical structures. Due to the complexity of each type of simulation it is often the case that a single package excels in either optical or electrical modelling, and the other remains a bottleneck. In this work, an efficient tool flow is described in order to combine the highly effective optical simulator Lumerical with the excellent fabrication and electrical simulation capability of Sentaurus. Interfacing between the two packages is achieved through tool command language and Matlab, offering a fast and accurate electro-optical characteristics of nano-structured PV devices.

#### Program summary

*Program title:* Interfacing\_Lumerical\_Sentaurus  
*Catalogue identifier:* AEWK\_v1\_0  
*Program summary URL:* [http://cpc.cs.qub.ac.uk/summaries/AEWK\\_v1\\_0.html](http://cpc.cs.qub.ac.uk/summaries/AEWK_v1_0.html)  
*Program obtainable from:* CPC Program Library, Queen's University, Belfast, N. Ireland  
*Licensing provisions:* Standard CPC licence, <http://cpc.cs.qub.ac.uk/licence/licence.html>  
*No. of lines in distributed program, including test data, etc.:* 4525  
*No. of bytes in distributed program, including test data, etc.:* 23729  
*Distribution format:* tar.gz  
*Programming language:* TCL, Matlab, Lumerical FDTD Solutions Version 8.7.3, TCAD Sentaurus Version j-2014.09.  
*Computer:* A multi-core, high ram workstation is recommended for running Lumerical Solutions and TCAD Sentaurus. The scripts provided here were run on a HPZ820 workstation with 2 X Intel Xeon E5-2680 2.70Ghz processors and 128GB DDR3-1600 RAM.  
*Operating system:* Linux.  
*Number of processors used:* Matlab scripts can be parallel processed. The scripts have been tested on 16 CPUs (32 Threads).  
*RAM:* For the TCL files, minimal RAM is needed. For the matlab script, it depends on the structure. The scripts have been tested using an upper limit of 128 GB.  
*Classification:* 4, 6, 18.  
*Nature of problem:*  
 Create a tool flow that models complex fabrication techniques, as well as accurate and efficient optical and electrical simulations for photovoltaic simulations.  
*Solution method:*  
 Code is provided to interface between Lumerical and Sentaurus using TCL and Matlab script.  
*Running time:*  
 Depends on structure complexity and number of processors used.

© 2015 The Authors. Published by Elsevier B.V.  
 This is an open access article under the CC BY license  
 (<http://creativecommons.org/licenses/by/4.0/>).

<sup>☆</sup> This paper and its associated computer program are available via the Computer Physics Communication homepage on ScienceDirect (<http://www.sciencedirect.com/science/journal/00104655>).

<sup>\*</sup> Corresponding author.

E-mail address: [tasmiat.rahman07@imperial.ac.uk](mailto:tasmiat.rahman07@imperial.ac.uk) (T. Rahman).

## 1. Introduction

Advances in photovoltaics (PV) in the last decade has been at an expeditious pace, covering new technologies such as thin film Si, dye sensitised PV, organic PV, nanowires, and most recently perovskite PV [1–5]. Given the rapid nature of PV development, whereby processing is central, the need to minimise time and costs

is crucial. As such, Technology Computer Aided Design (TCAD) tools help to simulate devices prior to processing in order to explore and optimise variables [6–9]. This can lead to observable trends in performance which can be used to determine suitable designs before fabrication. The modelling of PV can be separated into three elements: processing, optical and electrical characteristics. A multitude of packages exist to model these, including Sentaurus, Lumerical, Silvaco, Comsol, Crosslight and Cogenda to name a few [10–16]. Sentaurus TCAD is a comprehensive suite of modelling tools, and an industry standard for semiconductor processing and device simulation of complex geometry structures. However, it can also be useful to incorporate optical results from external packages into the Sentaurus suite. For optical modelling, Lumerical has more recently grown to an immensely popular FDTD package, as shown by the number of papers (>100) published utilising this tool since 2010 [17]. Alongside commercial packages such as Lumerical, accurate open source FDTD solvers are also available in the field, including MEEP [18]. In this work, Lumerical is integrated with Sentaurus TCAD to establish an efficient and easy to use tool flow which will allow researchers to explore innovative 3D PV devices. Whilst both packages contain optical and electrical simulation tools, they offer optimum performance and versatility in one of the two tasks. Current approaches to ameliorate this issue has involved utilising the Sentaurus structure editor to define new fields within a device [19]. These new data fields will then incorporate the external data. This paper provides an alternative method by manipulating the optical generation data files formed using Sentaurus Device. Furthermore, the work here extends to 3D devices that can be designed using the Sentaurus SProcess tool. As such, the integration of both packages allows the user a powerful tool that provides the accuracy and efficiency needed for intricate nano-scale PV modelling.

## 2. Tools

### 2.1. TCAD

Many tools are available in the Sentaurus Suite [20], however the use of SProcess to fabricate the device and then SDevice to solve the electrical transport equations is sufficient for most PV structures.

SProcess simulates processing steps such as deposition (e.g. spin-on-dopants), thermal annealing and etching, using various meshing strategies to generate a mixed grid element mesh [21]. This is advantageous as 3D structures can be formed from material growth and etching rather than explicit geometry definition. This allows a means of forming complex 3D structures through lithography steps followed by impurity diffusion as a function of time and temperature—key processing steps that are common to PV fabrication [22].

The development of PV technology is often pushed by advances in material science and as such Sentaurus has an ability to define new materials (alloys, polymers, perovskites, etc.). These are defined by first inheriting properties of materials in the database which can then be overwritten with published data.

Throughout the processing stage, and in preparation for the electrical solve, the Sentaurus package implements various meshing strategies to maintain a balance between accuracy of results and simulation time. The mesh forms boundary conditions for numerical calculations (e.g. Poisson equations) in the simulated device. The mesh algorithm can be achieved in both a static manner, in which predefined refinement windows are set with fixed mesh size, or a more complex adaptive method can be implemented to achieve meshing as a function of a chosen parameter (e.g. change in carriers density or electric field). For PV structures, the doping profile is a good measure to ensure the mesh is refined appropriately.

This will ensure that junction areas are finely meshed whereas bulk regions, where minimal change is observed, will have a more coarse mesh. Material interfaces (e.g. metal–semiconductor junctions or organic–inorganic heterojunction) should also be bounded by fine mesh constraints in order to achieve convergence in the simulation.

Sentaurus Device simulates the electrical behaviour in a semiconductor device that is represented as a mesh grid file [23]. For PV devices, the input grid file should contain the geometry of the structure, the doping profile and optical generation profile. Using this data, terminal currents and voltages are solved numerically based on physical device equations that describes the carrier distribution and conduction mechanisms. The key computation in the device simulation is to calculate the electrostatic potential determined by mobile (electrons and holes) and stationary charges (ionised dopants or traps). The simulator solves this using the Poisson equation.

When simulating a semiconductor device (both inorganic and organic), there are a vast amount of physical models to consider. Mobility and recombination models are two in particular that have significance in PV simulations. The doping dependent mobility model takes into account degradation due to impurity scattering in doped materials. In addition to this, surface phonon and surface roughness are also accounted for by considering mobility degradation at interfaces. For recombination, Shockley-read-hall, radiative, and trap assisted Auger recombination are accounted for [23].

### 2.2. Lumerical

For PV simulations, the modelling of light propagation through various media as well as scattering from interfaces is a crucial step and several approaches are available, each with a trade-off between computational load and accuracy. As PV technologies push further towards thin films and nanoscale structures, methods such as Raytracing, which provide solutions based on geometric optics alone, are no longer applicable for accurate results when wavelengths are comparable to the feature size. Current approaches to compute nanoscale optics require solving Maxwell's equations. A variety of methods exist to solve these equations, including Finite Difference Time Domain (FDTD) method, Finite Element Method (FEM), Transfer Matrix Method (TMM) and Rigorous Coupled-Wave Analysis (RCWA), to name a few. For PV simulation whereby the injected wave has broadband wavelength range, the FDTD method is most efficient. Lumerical, like many commercial optical solve packages, uses this method [17].

The FDTD method solves Maxwell's equations in the time domain. In this approach, both space and time are segmented into discrete sectors. Space is divided into cuboid cells whereby the electric fields are located on the edges of the cell and the magnetic fields are found on the faces. Furthermore, time is discretised into small steps where each step represents the time required for the field to propagate between adjacent cells. A leapfrog scheme is used to update the electric and magnetic fields as a function of time. Through this method it can obtain complex-valued fields and normalised transmissions as a function of frequency.

The key input parameters to consider for the simulation are the material properties, light sources, data monitors, boundary conditions and also meshing. When using dispersive media, as is the case for PV devices, a fitted model of multi-coefficients is used to represent tabulated refractive index ( $n, k$ ) data. Various types of sources exist to excite the structures within the simulation domain such as: Gaussian source, TFSF and plane wave. The latter is used to model uniform electromagnetic energy with wavelength range (300 nm–1000 nm) injecting from one side of the simulation domain. Structures tend to have a periodicity and therefore the boundary conditions are periodic in the  $x$  and  $y$  direction, whilst

the  $z$  direction have perfectly matched layers to absorb any reflected and transmitted fields. Furthermore, in many instances, the structure is also symmetric as well as periodic. Under these conditions we incorporate symmetric and antisymmetric boundaries to reduce computation time.

In addition to the boundary condition, the quality of the mesh will also affect the accuracy of results. The mesh is a Cartesian grid which represents the structure. For each mesh point, the material and geometrical information is stored and electric and magnetic fields are solved. As such, a trade-off exists between a fine mesh (i.e. a smaller minimum mesh length) and computation time. A meshing algorithm is applied by the solver to form a mesh as a function of the material refractive index and structure interface.

### 2.3. Comparison

Both Lumerical and Sentaurus provide tools for structure generation, optical modelling and electrical modelling. However, integrating the two removes the bottlenecks of each package and utilises the advantages.

#### 2.3.1. Structure generation

Whilst Lumerical has a comprehensive library of structures from which to build the device, it lacks the freedom and versatility to define unique designs based on material processing chemistry. This is of particular importance in PV as complex 3D doping profiles can be modelled rather than pre-defined. The ability for Sentaurus to replicate fabrication processes using elaborate meshing strategies, is based upon decades of experience in modelling semiconductor devices [20].

#### 2.3.2. FDTD Optical modelling

Sentaurus provides an electromagnetic wave (EMW) solver that also uses the FDTD method [24]. However, Lumerical shows enhanced simulation time efficiency as observed in Fig. 1. The simulations were performed on a silicon nanowire array whereby all parameters, including boundary conditions, mesh density and termination criteria are kept consistent. These results show that Lumerical is more efficient and has negligible dependence on the discrete Fourier transform (DFT) resolution (i.e. number of wavelengths measured). Furthermore, for this example, due to the simplicity of the structure Lumerical works more efficiently in single-core than in multi-core. This however, is not observed in the Sentaurus case. Potentially, Lumerical can outperform further by using symmetry and antisymmetry boundaries in  $x$  and  $y$  (this exploits the symmetry of these structures and quarters the simulation domain).

The Lumerical package has also proven to provide more consistent optical results for broadband wavelength simulations compared to that of the Sentaurus EMW solver. An error noted by Sentaurus on their internal site, as a code defect in calculating the discrete Fourier transform (DFT) phase factors, may be the root cause of this inaccuracy in DFT simulations. As a result, optical quantities extracted from EMW simulations using DFT can exhibit errors compared to continuous wave results [25]. To illustrate the error observed, Fig. 2 compares the power flux density through a reflection data monitor for both cases. To circumvent this problem, Synopsys advise to either use a sequence of single-wavelength continuous wave simulations instead of a single DFT simulation for multiple wavelengths, or else create user-defined dispersive model poles to produce better fitting of the complex refractive index data [25]. The newest version of the Sentaurus EMW solver provides a visual fitting tool to aid in the latter process. Whilst this may provide a suitable workaround to improve accuracy, it can be a complex step in performing FDTD modelling. Furthermore, the ease of use of Lumerical surpasses that of Sentaurus due to its graphical user interface (GUI) whereas the Sentaurus EMW solver is purely code based [24].

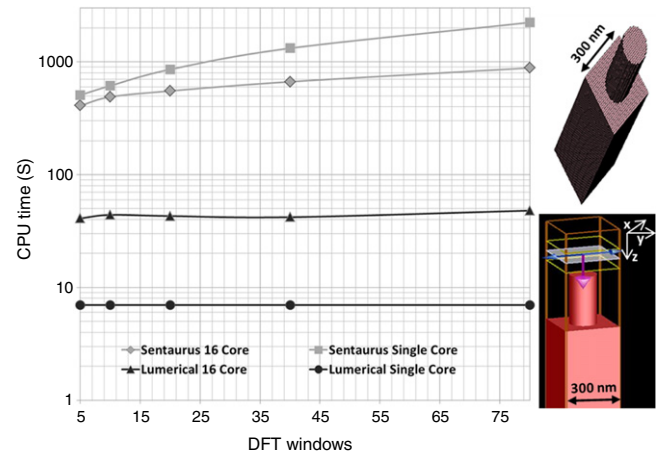


**Fig. 1.** Comparison of simulation times using multi-core and single-core for Lumerical and Sentaurus Packages. The simulation is of a basic periodic silicon nano-wire array formed from a cylinder and a cuboid. The nano-wire has a radius of 75 nm and a height of 500 nm, whilst the bulk region has dimension of 300 nm × 300 nm × 1 μm. A mesh density of 10 nm is set. The boundaries are periodic in  $x$  and  $y$ , and PML in  $z$ . The structure formed in Sentaurus is shown on the top-right (plotted with SVisual tool), whilst the simulation domain for Lumerical is shown on the bottom-right (plotted with Lumerical Visualiser).

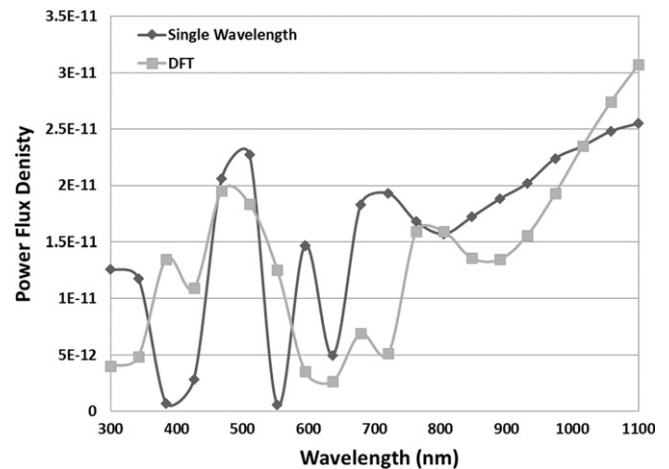


**Fig. 2.** Comparison of reflected power flux density on Silicon nanowire using DFT and single-wavelength simulation with the Sentaurus EMW solver.

#### 2.3.3. Electrical modelling

The Sentaurus Device package is a more advanced electrical modelling package compared to that of Lumerical Device. It provides a more comprehensive physical model database as well as greater choice with respect to numerical solving algorithms. This provides not only more efficient electrical modelling but the ability to analyse a far greater amount of device parameters [23].

## 3. Integration

The principle behind the tool flow is the ability for SDevice to run an electrical solve using optical solve data from previous simulations. It does this by reading an input file known as 'optical generation input file (OGI.TDR)'. SDevice reads this TDR file that contains optical generation data and interpolates it to the geometry and doping data also provided, to run optoelectronic simulations. This means that if the optical solve data from Lumerical can be written to a TDR file, then it can be used in SDevice.

As such, the process is as follows: The structure is formed using SProcess; this structure is used in SDevice to run purely electrical simulations and therefore give dark IV characteristics. The tool at

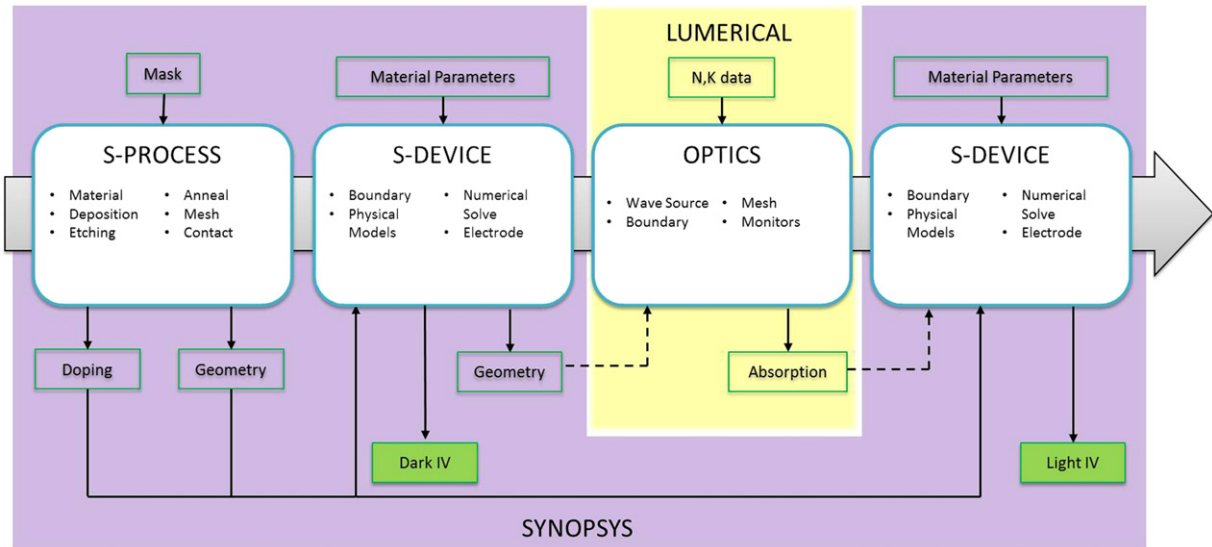


**Fig. 3.** An overview of the tool flow used in this work. The key input and output files are shown, as well as the main packages which are called upon and its order of use. The dashed line represents the use of TCL language and Matlab script to interface the files between Sentaurus and Lumerical.

this stage is also used to produce an ‘optical generation output (OGO)’ file. Whilst no optical solve is executed, it will produce an OGO.TDR, with zero for carrier generation but containing the necessary coordinate information, that is used as the template on which to write Lumerical data. Once Lumerical data is written onto this OGO.TDR file, this then becomes an optical generation input file (OGI.TDR) at the second stage of SDevice.

### 3.1. Tool flow

The tool flow can be seen in Fig. 3. The four main tools used, are SProcess, SDevice, Lumerical and finally SDevice again. To illustrate the use of this tool flow, a hybrid silicon pyramid-nanowire array structure is modelled [26], as this utilises many of the useful steps that are provided for PV simulation. The full script used to form this structure on SProcess and model on SDevice are provided in the program library. The following shows pseudo-code for descriptive purposes that readers can apply for their own use.

The first tool used, is SProcess.

```

1 Initialise Silicon structure
2 Etch Pyramid{
3   Grow Oxide
4   Deposit Resist
5   Apply Mask and expose (read from Mask file)
6   Etch Oxide
7   Strip Resist
8   Apply crystallographic etch on Silicon
9   Etch Oxide}
10 Etch Nanowires{
11  Deposit Resist
12  Apply Mask and expose (read from Mask file)
13  Apply anisotropic etch on Silicon
14  Strip Resist}
15 Apply Mesh algorithm
16 Dope structure{
17  Deposit spin-on-dopant (e.g. Phosphorous)
18  Thermally anneal structure to diffuse dopants
19  Etch grown oxide}
20 Define Contacts
21 Save structure (SPROCESS.TDR)

```

This tool works by first defining an initial silicon substrate, followed by the various fabrication steps to build the structure. This often involves a mask file that is used for lithography steps. Meshing strategies are defined to ensure accurate processing and future convergence in device simulation. Contacts are defined as the

last step. The output data is of TDR format, and contains a multitude of datasets (e.g. doping concentration, geometry, stress, etc.) that completely describe the geometry and material parameters at equilibrium.

The second tool is SDevice.

```

1 Set input data{
2   Grid = SPROCESS.TDR
3 }
4 Set output data{
5   Plot = FULL_PLOT.TDR
6   Current = DARK_IV.PLT
7   OpticalGenerationOutput = OGO.TDR
8 }
9 Set data fields to plot {
10  Doping Profiles, Band structure
11  Carrier Densities, Currents, Traps
12  Fields, Potentials and Charge distributions
13  Generation/Recombination, Optical Generation
14  ...
15 }
16 Define Electrodes
17 Define Physics models{
18  Traps
19  Recombination{
20    Shockley-Read-Hall, Auger
21    Radiative, Surface
22  }
23  Mobility
24 }
25 Set Iterative method and power{
26  Newton/Gummel
27  Number of CPU
28 }
29 Apply electrical sweep{
30  Quasistationary Voltage Start, Step, End
31  Solve Poisson for electrons and holes
32 }

```

This stage is to use the output structure from SProcess to run current–voltage (IV) simulation without any light absorption. This will give the IV characteristics in the dark and also produces an optical generation output TDR file. The SDevice command file takes in the geometry and doping data from SProcess and applies a numerical solve. It implements specified device physics models from a comprehensive database. User-defined material parameters can overwrite default parameters to account for more recent published or in-house experimental data (e.g. surface recombination velocity for nanowire–air interfaces). A full output TDR file is also produced



and this contains all the specified plot data (e.g. electric fields, carrier generation profile, current density, mesh, etc.).

The third tool is Lumerical.

```

1 Import structure{
2   Binary file = OGO.TXT
3   Refractive index = Published tabulated data
4 }
5 Define simulation domain{
6   Mesh Accuracy
7   Boundary conditions{
8     Periodic
9     Anti-Symmetric, Symmetric
10    Perfectly Matched Layers
11    Termination Criteria
12  }
13 Define source wave{
14   Type = Plane
15   Wavelength range = 300 nm--1000 nm
16   Location = plane above structure
17 }
18 Define monitors{
19   Reflection monitor{
20     2D
21     Location = plane above source wave
22   }
23   Absorption monitor{
24     3D
25     Downsampling
26     Location = boxes covering structure
27   }
28 Set CPU/Memory power

```

The Lumerical tool which is sandwiched in-between the two SDevice packages imports the structure from the output data of the first SDevice simulation. Whilst the complex 3D structure can be imported from Sentaurus tools, simpler structures can be reconstructed without any importation using Lumerical's own structure editor. This tool can also make use of the mask file as both packages utilise the industry standard GDS format. Once the structure is imported, the refractive index data of the materials is also required. The structure is then re-meshed depending on the simulation constraints.

The three key elements to the simulation are the injected wave source, the boundary conditions and the monitors used. The latter determines the output data. For PV simulations a key monitor is an analysis group 'solar generation'. This outputs a spatial carrier generation profile of the structure in a MAT file. For very complex structures that require fine meshing, often the output files are too computationally intensive, limited by read access memory (RAM) to calculate in one simulation. As such, the monitor can be down-sampled such that adjacent mesh cells are averaged, or often the simulation is run numerous times and each time the monitor is confined to a different section of the structure. As a smaller number of cells are now computed, less RAM is required. The total generation profile is then merged from the numerous monitor files.

The final stage is SDevice

```

1 Set input data{
2   Grid = SPROCESS.TDR
3   OpticalGenerationInput = OGI.TDR
4 }
5 Set output data{
6   Plot = FULL_LIGHT_PLOT.TDR
7   Current = LIGHT_IV.PLT
8 }
9 ...
10 ...
11 Define Physics models{
12   Traps
13   Recombination{
14     Shockley-Read-Hall, Auger
15     Radiative, Surface
16   }
17   Mobility
18   Optics{

```

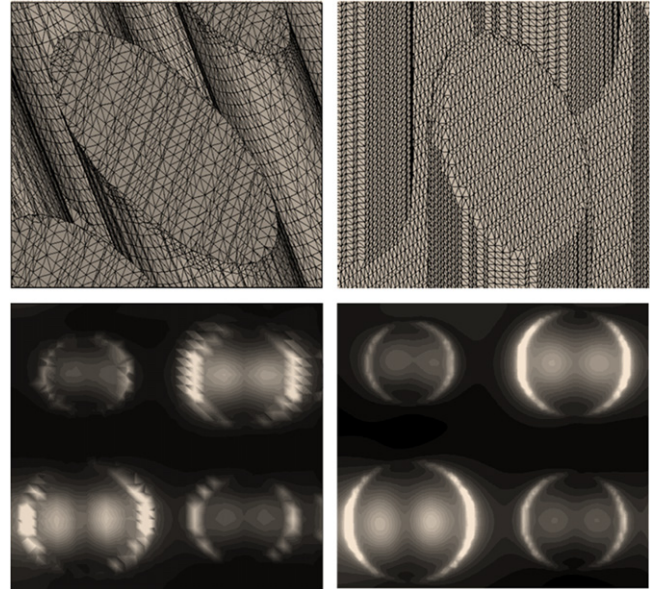


**Fig. 4.** Top: Comparison of mesh quality between Delaunay mesh in Sentaurus (left) and Cartesian mesh in Lumerical (right). Bottom: Comparison of the optical carrier generation data, after mapping from Lumerical (right) to Sentaurus (left). The images for Sentaurus are plotted in SVisual and for Lumerical in Matlab.

```

19   ReadFromFile=OpticalGenerationInput
20   }
21 }
22 ...
23 ...
24 Apply electrical sweep{
25   Transient{
26     Gradual increase to OGI data
27     Time start, step, end
28   }
29   Quasistationary Voltage Start, Step, End
30   Solve Poisson for electrons and holes
31 }

```

This stage is the IV simulation under illumination. It uses the already processed OGI.TDR file and interpolates the carrier generation data. Since geometry from this will match that of SPROCESS.TDR exactly, there is negligible error. Therefore, no optical solve is undertaken using SDevice in this tool flow, only its ability to take in carrier generation data from a TDR file. Since this simulation generates a large current density at the initial guess of the electrical solve (0 V), an initial transient simulation is undertaken before the quasi-stationary voltage sweep.

### 3.2. TCAD-Lumerical interface

The integration of the two separate packages is achieved by data extraction using a TCL language script and data mapping using a MATLAB script. In this section the pseudo-code is shown, such that other languages can be used, however the full script is available within the program library. See Fig. 4 for a comparison of the mesh and the carrier generation profile after mapping between Sentaurus and Lumerical.

#### 3.2.1. File types

As mentioned previously, the standard file format throughout TCAD Sentaurus is TDR. It contains various datasets (e.g. dopant concentration) for every state (for transient simulations), region and geometry of the structure. To import the structure to Lumerical, the coordinate data must be in a TXT file format. The output of Lumerical (i.e. spatial absorption profile) is in a MAT file. Finally, for post data mapping, the absorption data must be written into the TDR format for use in SDevice.

### 3.2.2. *Sentaurus to lumerical*

The first step is to access the TDR file and unfold the data into a format that is readable by external packages such as Lumerical. The TDR file in this case is the optical generation output after the first stage of SDevice. This has no optical solve and as such the dataset 'optical generation' will have a zero value. However, this file is useful as it contains the relevant coordinate list for optical modelling. The aim is to extract this coordinate list into a data form that can be read by Lumerical.

```

1 set input file {
2     Input = OGO.TDR,
3     permission = "read"
4 }
5 set output file {
6     Output = OGO_coordinates.TXT
7     permission = "write"
8 }
9 Find number of datasets {
10    Specify location in TDR{
11        Geometry, Region, State
12    }
13    Get number of datasets
14 }
15 Find coordinate data {
16    For all datasets{
17        find those that contain 'optical generation
18        ' quantities
19        extract x,y and z coordinate
20        save coordinate to 'coordinate list'
21    }
22 Write 'coordinate list' to 'OGO_coordinate.TXT'

```

This process is necessary as it extracts the coordinates of the simulation space that is relevant for optical modelling. This data can be reconstructed such that the structure is reproducible in Lumerical. The import function in Lumerical requires a binary list whereby 1 and 0 represent the presence and absence of material, respectively. This list refers to the geometrical location ( $X_1, Y_1, Z_1$ ) to ( $X_j, Y_k, Z_l$ ) where  $j, k$  and  $l$  are last indices in each respective plane. The following code is used for this purpose:

```

1 set input data{
2     structure_xyz = Read 'OGO_coordinate.TXT'
3 }
4 create full coordinate list {
5     find all unique coordinates x,y,z
6     define mesh density factor Nx,Ny,Nz
7     list all possible combinations of x,y,z
8 }
9 create binary list {
10    for all rows in full coordinate list{
11        if coordinates match input data
12        then write 1 to binary_list
13        else write 0 to binary_list
14    }
15 }
16 Write 'binary_list' to 'binary_list.TXT'

```

This essentially creates a coordinate list for a Cartesian grid with uniform spacing in each plane. The density of this depends on the values of the mesh density factors ( $N_x, N_y$  and  $N_z$ ). When equal to 1, this will represent a grid density which ensures no loss of data when replicating the structure in Lumerical. As these values increase, there is some loss in data but any degradation in the replica will depend on the complexity of the structures. In cases of simple structures on a low RAM computer, increasing these numbers maybe beneficial.

Through the aforementioned process of importing a TCAD device into Lumerical, only the geometry of the structure is specified. Its material properties (i.e. optical constants) are then defined within Lumerical. Therefore, different materials within a TCAD device are imported into Lumerical as different structures and

then their material properties defined accordingly. When extracting/reading the structure data from TCAD as well as writing into the structure data in TCAD, it is crucial to attain which material/region is being read/written. To identify this, the code in file 'TDR\_check' is used. This code is supplied by Synopsys and is used for identifying regions and materials within a structure.

### 3.2.3. *Lumerical to sentaurus*

The output of the Lumerical simulation is a 3D matrix data representing the carrier generation profile within the whole simulation domain. In order to map this 3D profile to the structure back in TCAD, the first stage is to list the carrier generation data for each coordinate that exists for the structure. This data will then be written into the TDR format.

```

1 set input data{
2     structure_xyz = Read 'OGO_coordinate.TXT'
3     absorption_profile {
4         Read 'lumerical_1.MAT'
5         Read 'lumerical_2.MAT'
6         Read 'lumerical_3.MAT'
7         ....
8     }
9 For the number of rows in structure_xyz{
10    match coordinates in absorption_profile{
11        limit search space{
12            check if coordinate exists in MAT
13            file 1,2,3..
14        }
15        find minimum distance {
16            absorption_data(x,y,z)-structure_xyz(
17                x,y,z)
18        }
19        Extract absorption data
20    }
21    if absorption data < 1 {
22        increase search space
23    until absorption data found
24    extract absorption data
25    }
26 }
27 Write absorption data to OGI.TXT file.

```

The aim of Lines 14–18 is to match the geometric points of the Lumerical structure to the Sentaurus structure. This is achieved by searching for the minimum distance between a given point from a Lumerical absorption profile, and a data point from the desired Sentaurus structure. Lines 19–23 are used to ensure that at an air-structure interface, the surface of the TCAD structure takes the data of absorbed material in Lumerical and not the air material. This is achieved by first checking if the absorption data taken for the nearest matching coordinate is negligible, i.e. less than 1. If this is the case, then a search method begins whereby the search space grows by one mesh cell in all directions until the nearest absorption cell is found.

Once the absorption data has been collated into a list corresponding to the structure coordinates, it is then written onto the TDR file. Since the coordinate list is taken from the structure post-device, it is a simple process of overwriting the carrier generation (currently 0 after "dark" simulation) for each location. This TDR file then assumes an illuminated structure and the IV simulation can be undertaken.

```

1
2 set input file {
3     Input = OGI.TXT,
4     permission = "read"
5 }
6 set output file {
7     Output = OGI.TDR
8     permission = "write"
9 }
10 Find number of datasets {
11    Specify location in TDR{

```

```

12     Geometry, Region, State
13     }
14     Get number of datasets
15     }
16 Overwrite Absorption data {
17     For all datasets{
18         find those that contain 'optical generation
19         ' quantity
20         overwrite data quantity with Input data
21     }

```

The key here is that the number and order of coordinates in the TDR and TXT file must match.

#### 4. Conclusion

In this work an efficient tool flow is described in-order to integrate Lumerical, an efficient FDTD optics solver, into TCAD Sentaurus, an industry standard for electrical simulation. When combined, a complete package exists for broadband optoelectronic modelling (ideal for PV). This allows the benefits of material processing chemistry to form structures, followed by accurate and computationally efficient FDTD modelling, and finally electrical characterisation using a comprehensive database of device physics models. In order to integrate the two packages, the ability for Sentaurus to read previously solved optical generation data is manipulated. An electrical solve is undertaken with no illumination, this will output a carrier generation file with zero data. This file is used for two purposes, firstly to form the structure on Lumerical, and secondly to transfer the output data back into Sentaurus. The interface between the two packages is achieved with a combination of tool command language and Matlab script, both of which can be used in open-source platforms.

#### Acknowledgements

T.R. is supported by a EPSRC Standard Research Student (DTG) (EP/J500239/1) doctoral training award from Imperial College London. The authors would like to thank the technical support provided by Lumerical Solutions Inc. and Synopsys Inc.

#### References

- [1] S. Kim, J.-W. Chung, H. Lee, J. Park, Y. Heo, H.-M. Lee, Remarkable progress in thin-film silicon solar cells using high-efficiency triple-junction technology, *Sol. Energy Mater. Sol. Cells* 119 (2013) 26–35.
- [2] I. Chung, B. Lee, J. He, R.P. Chang, M.G. Kanatzidis, All-solid-state dye-sensitized solar cells with high efficiency, *Nature* 485 (7399) (2012) 486–489.
- [3] W.S. Koh, M. Pant, Y.A. Akimov, W.P. Goh, Y. Li, Three-dimensional optoelectronic model for organic bulk heterojunction solar cells, *IEEE J. Photovolt.* 1 (1) (2011) 84–92.
- [4] B. Williams, A. Taylor, B. Mendis, L. Phillips, L. Bowen, J. Major, K. Durose, Core-shell ito/zno/cds/cdte nanowire solar cells, *Appl. Phys. Lett.* 104 (5) (2014) 053907.
- [5] M.A. Green, A. Ho-Baillie, H.J. Snaith, The emergence of perovskite solar cells, *Nat. Photonics* 8 (7) (2014) 506–514.
- [6] Y. Xing, P. Han, S. Wang, Y. Fan, P. Liang, Z. Ye, X. Li, S. Hu, S. Lou, C. Zhao, et al., Performance analysis of vertical multi-junction solar cell with front surface diffusion for high concentration, *Sol. Energy* 94 (2013) 8–18.
- [7] M.G. Deceglie, V.E. Ferry, A.P. Alivisatos, H.A. Atwater, Accounting for localized defects in the optoelectronic design of thin-film solar cells, *IEEE J. Photovolt.* 3 (2) (2013) 599–604.
- [8] A. Kanevce, T.A. Gessert, Optimizing cdte solar cell performance: impact of variations in minority-carrier lifetime and carrier density profile, *IEEE J. Photovolt.* 1 (1) (2011) 99–103.
- [9] N. Huang, M.L. Povinelli, Design of passivation layers on axial junction gas nanowire solar cells, *IEEE J. Photovolt.* 4 (6) (2014).
- [10] M.M. Wilkins, A. Boucherif, R. Beal, J.E. Haysom, J.F. Wheeldon, V. Aimez, R. Ares, T.J. Hall, K. Hinzer, Multijunction solar cell designs using silicon bottom subcell and porous silicon compliant membrane, *IEEE J. Photovolt.* 3 (3) (2013) 1125–1131.
- [11] Y. Xu, J.N. Munday, Light trapping in a polymer solar cell by tailored quantum dot emission, *Opt. Express* 22 (102) (2014) A259–A267.
- [12] F. Sgrignuoli, G. Paternoster, A. Marconi, P. Ingenhoven, A. Anopchenko, G. Pucker, L. Pavesi, Modeling of silicon nanocrystals based down-shifter for enhanced silicon solar cell performance, *J. Appl. Phys.* 111 (3) (2012) 034303.
- [13] R. Jeyakumar, T. Maiti, A. Verma, Influence of emitter bandgap on interdigitated point contact back heterojunction (a-si: H/c-si) solar cell performance, *Sol. Energy Mater. Sol. Cells* 109 (2013) 199–203.
- [14] K. Zhou, S.-W. Jee, Z. Guo, S. Liu, J.-H. Lee, Enhanced absorptive characteristics of metal nanoparticle-coated silicon nanowires for solar cell applications, *Appl. Opt.* 50 (31) (2011) G63–G68.
- [15] Z. Li, M. Lestradet, Y. Xiao, S. Li, Effects of polarization charge on the photovoltaic properties of ingan solar cells, *phys. Status Solidi (a)* 208 (4) (2011) 928–931.
- [16] F. Wang, H. Yu, J. Li, S. Wong, X.W. Sun, X. Wang, H. Zheng, Design guideline of high efficiency crystalline si thin film solar cell with nanohole array textured surface, *J. Appl. Phys.* 109 (8) (2011) 084306.
- [17] <https://www.lumerical.com/>, accessed 4 November, 2014.
- [18] A.F. Oskooi, D. Roundy, M. Ibanescu, P. Bermel, J.D. Joannopoulos, S.G. Johnson, Meep: A flexible free-software package for electromagnetic simulations by the ftd method, *Comput. Phys. Comm.* 181 (3) (2010) 687–702.
- [19] M.D. Kelzenberg, Silicon Microwire Photovoltaics, Appendix B (Ph.D. thesis), California Institute of Technology, 2010, URL [http://mkelzenb.caltech.edu/thesis/mk\\_thesis\\_appB.pdf](http://mkelzenb.caltech.edu/thesis/mk_thesis_appB.pdf).
- [20] <http://www.synopsys.com/tools/tcad/Pages/default.aspx>, accessed 4 November, 2014.
- [21] Synopsys, Mountain View, CA 94043, Sentaurus Process User Guide, j-2014.09 ed., Dec. 2014.
- [22] T. Rahman, K. Fobelets, Simulation of rough silicon nanowire array for use in spin-on-doped pn core-shell solar cells, in: *Modelling Symposium (EMS), 2013 European*, IEEE, 2013, pp. 725–729.
- [23] Synopsys, Mountain View, CA 94043, Sentaurus Device User Guide, j-2014.09 ed., Dec. 2014.
- [24] Synopsys, Mountain View, CA 94043, Sentaurus Device Electromagnetic Wave Solver User Guide, j-2014.09 ed., Dec. 2014.
- [25] <https://solvnet.synopsys.com/>, accessed 4 November, 2014.
- [26] T. Rahman, M. Navarro-Cia, K. Fobelets, High density micro-pyramids with silicon nanowire array for photovoltaic applications, *Nanotechnology* 25 (48) (2014) 485202.